

Approaches to sorption modeling for high-level waste performance assessment

David R. Turner^{*}, Stephen A. Sassman

Center for Nuclear Waste Regulatory Analyses, San Antonio, TX 78228-0510, USA

Received 17 December 1993; accepted 15 December 1994 after revision

Abstract

Available experimental data indicate that radionuclide sorption is a complex function of mineral and solution chemistry. Surface complexation models (SCM's) can be used to describe this sorption behavior, but comparison of model results requires interpretation of these data using a consistent set of model parameters. Based on available potentiometric titration data, a uniform approach is used to develop a set of consistent parameters for three SCM's and nine simple (hydr)oxides. Using these parameters, all three models prove capable of reproducing observed charge data, but each model is subject to limitations. Binding constants are developed for the U(VI)–H₂O–CO₂–goethite system. In the absence of CO₂, all three models are able to reproduce observed trends for a given data set assuming a single surface complex. Two or more surface complexes were required to model observed sorption behavior in the presence of CO₂/CO₃²⁻. The experimental data from the two studies considered differ, and binding constants based on combining modeling results do not perform as well, exhibiting bias towards the larger data set. For more complex minerals, sorption of Np(V) on biotite and U(VI) on kaolinite were well modeled using the simplest SCM and assuming stoichiometric proportions of silanol (SiOH⁰) and aluminol (AlOH⁰) sites.

1. Introduction

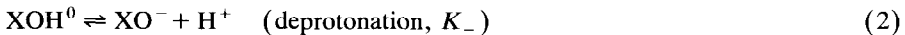
Surface complexation models (SCM's) have largely been developed and refined as a means of investigating the pH-dependent sorption behavior of toxic elements such as Zn²⁺, Cd²⁺, Pb²⁺ and CrO₄²⁻. Because of increasing concern with radioactive waste disposal, similar studies have begun to be performed for key radionuclides (especially actinides). To take full advantage of this research for performance assessment (PA),

^{*} Corresponding author.

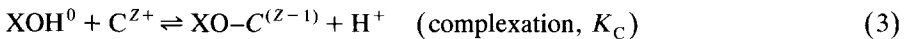
there is a need to apply SCM's to radionuclide sorption. This study has used a uniform approach to interpret available potentiometric titration data and develop a set of consistent parameters for commonly used SCM's for different simple (hydr)oxides. With these parameters in place, it will be possible to use SCM's to interpret existing data and to compare model performance in predicting radionuclide sorption on these minerals. It may also be possible to use the SCM approach to examine radionuclide sorption on more complex rock-forming minerals such as feldspar and mica.

2. Complexation models —general features

Three commonly used SCM's include the Diffuse Layer (DLM), Constant Capacitance (CCM) and Triple Layer (TLM) Models. Details of these models are given elsewhere (Davis and Kent, 1990; Westall and Hohl, 1980), and only a brief description is included here. The DLM and CCM each assume a single layer at the particle–water interface. As its name implies, the TLM assumes three layers. To describe the acid–base behavior of a mineral surface, all three models assume equilibrium reactions involving protonation/deprotonation of amphoteric surface functional groups (XOH^0) written in the form:



where K_+ and K_- are referred to as intrinsic surface acidity constants. An example of a typical general sorption reaction is:



where XOH^0 represents a neutral surface site; and C^{Z+} is a sorbing cation. The corresponding equilibrium constant for this reaction, K_C , is commonly called a sorption or binding constant. A similar construction is used for anion sorption. For mass action, activities of species such as H^+ and C^{Z+} near the surface are corrected for electrostatic effects using the exponential Boltzmann relation:

$$\{C^{Z+}\}_{\text{surface}} = \{C^{Z+}\}_{\text{bulk}} [\exp(-\Psi_J F/RT)]^Z \quad (4)$$

where Ψ_J is electrostatic potential (volts) of layer J , which depends on the model; F is the Faraday constant; and R and T are the ideal gas constant and temperature (in kelvins), respectively.

Mass balance for the total concentration of available surface sites (T_{XOH}) is described by:

$$T_{XOH} = [(N_S) \times (A_{SP}) \times (c_S) \times 10^{18} \text{ nm}^2 \text{ m}^{-2}] / 6.023 \cdot 10^{23} \text{ sites mol}^{-1} \quad (5)$$

where N_S is site density (sites nm^{-2}); A_{SP} ($\text{m}^2 \text{ g}^{-1}$) is specific surface area of the mineral; and c_S is the solid mass of the adsorbent in suspension (g L^{-1}). These mass action, mass balance and model-specific charge–potential relations can be used in a

manner analogous to that employed by geochemical speciation codes (Westall and Hohl, 1980; Allison et al., 1991).

Relative to empirical models, the strength of all SCM's is the ability to handle changes in chemistry quantitatively. The major drawback to the models is the complexity and nonlinearity inherent in their construction, which limits practical applications in PA. Each SCM requires several types of model-dependent parameters (up to eight for the TLM) to characterize the mineral–water interface. Parameter values are imperfectly known, and in practice have been used as multiple fitting parameters specific to a particular data set. Because of fundamental differences in how the models represent the mineral–water interface and the tendency to use data set-specific parameters, it is difficult to compare directly the results of different studies (Westall and Hohl, 1980). One recently advocated approach is the adoption of a “standard” set of parameters that is uniformly applied in all systems (Davis and Kent, 1990; Dzombak and Morel, 1990; Hayes et al., 1990). While this approach may not represent the exact processes operating at the interface, it limits the number of adjustable parameters and serves to establish baselines for future comparison of modeling results.

3. SCM parameter estimation using FITEQL, Version 2.0

Model-specific acidity constants were determined here by interpreting potentiometric titration data using the parameter optimization program FITEQL, Version 2.0 (Westall, 1982). The code requires details on mineral properties, mass balance and mass action for the chemical equilibrium model, and serial experimental data. An electronic digitizing tablet was used to convert graphical data to numerical values. For titration data, surface charge data were converted to total H^+ for input into FITEQL.

To consider mass-balance constraints on site availability, all SCM's require a single value for A_{SP} . However, surface area, generally determined by BET/ N_2 techniques (BET = Brunauer–Emmett–Teller adsorption isotherm), is subject to uncertainty depending on grain size, mineral preparation, outgassing of the sample prior to measurement, and mineral aging (Yates, 1975). The applicability of a surface area measured on dry samples in a vacuum to that in solution is also uncertain. In some cases, A_{SP} has been used as a fitting parameter (Hsi and Langmuir, 1985). Dzombak and Morel (1990) acknowledged these uncertainties and selected a single generalized surface area of $600 \text{ m}^2 \text{ g}^{-1}$ for ferrihydrite (amorphous ferric oxide). The methods of Dzombak and Morel (1990) have been followed here; based on reported measured values, a single generalized A_{SP} has been assumed for each mineral and applied consistently for each SCM considered (Table 1). Although information is undoubtedly lost in this simplification, the distinction in A_{SP} between minerals is maintained. In most cases the use of similar mineral preparation techniques between studies provides some support for this assumption. The difference between the generalized surface area and the reported surface area is on the order of 10–20% in most instances, probably within the limits of uncertainty on the measurement itself. One exception has been the titration data for anatase. In this case, the relative difference in reported surface area between the studies of Berube and

Table 1
Best estimate values for SCM constants — Simple (hydr)oxides

Mineral	Mineral properties ^a	Reference(s)	Model	$\log K_+$ ($\pm 95\%$) ^b	$\log K_-$ ($\pm 95\%$) ^b	$\log K_{\text{anion}}$ ($\pm 95\%$) ^b	$\log K_{\text{cation}}$ ($\pm 95\%$) ^b
Goethite	$\text{pH}_{\text{ZPC}} = 8.0$ $A_{\text{SP}} = 50 \text{ m}^2 \text{ g}^{-1}$	Yates and Healy (1975), Balistreri and Murray (1981), Hsi and Langmuir (1985), Hayes et al. (1990), Mesuere (1992)	CCM (0.1 M)	6.47 ± 0.72	-9.03 ± 0.22	n.a.	n.a.
			DLM	7.35 ± 0.11	-9.17 ± 0.08	n.a.	n.a.
			TLM ^d	6.00	-10.00	8.78 ± 0.13	-7.64 ± 0.07
Ferritic drite ^c	$\text{pH}_{\text{ZPC}} = 8.0$ $A_{\text{SP}} = 600 \text{ m}^2 \text{ g}^{-1}$	Yates (1975), Davis (1977), Swallow (1978), Hsi and Langmuir (1985)	CCM (0.1 M)	7.35 ± 1.08	-8.45 ± 2.23	n.a.	n.a.
			DLM	7.29 ± 0.10	-8.93 ± 0.07	n.a.	n.a.
			TLM ^d	6.00	-10.00	8.43 ± 0.04	-7.66 ± 0.12
Magnetite	$\text{pH}_{\text{ZPC}} = 6.7$ $A_{\text{SP}} = 5 \text{ m}^2 \text{ g}^{-1}$	Regazzoni et al. (1983)	CCM (0.1 M) ^e	6.26	-7.32	n.a.	n.a.
			DLM	6.72 ± 0.02	-6.37 ± 0.71	n.a.	n.a.
			TLM ^d	4.70	-8.70	7.95 ± 0.11	-5.47 ± 0.06
SiO_2	$\text{pH}_{\text{ZPC}} = 2.8$ $A_{\text{SP}} = 175 \text{ m}^2 \text{ g}^{-1}$	Bolt (1957), Abendroth (1970)	CCM (0.1 M)	(^f)	-7.04 ± 0.09	n.a.	n.a.
			DLM	(^f)	-7.20 ± 0.05	n.a.	n.a.
			TLM ^d	0.90	-4.90	(^f)	-6.22 ± 0.05
$\alpha\text{-Al}_2\text{O}_3$	$\text{pH}_{\text{ZPC}} = 8.9$ $A_{\text{SP}} = 12 \text{ m}^2 \text{ g}^{-1}$	Hayes et al. (1990)	CCM (0.1 M) ^e	8.12	-9.56	n.a.	n.a.
			DLM	8.33 ± 0.15	-9.73 ± 0.12	n.a.	n.a.
			TLM ^d	6.90	-10.90	10.12 ± 0.03	-7.73 ± 0.07

γ -Al ₂ O ₃	pH _{ZPC} = 8.4 A _{SP} = 120 m ² g ⁻¹	Huang and Stumm (1972), Sprycha (1989)	CCM (0.1 M)	n.a.	n.a.	n.a.	n.a.
			DLM	6.92 ± 0.06	-9.00 ± 0.15	8.28 ± 0.05	n.a.
			TLM ^d	6.85 ± 0.06	-9.05 ± 0.09	n.a.	n.a.
δ -MnO ₂	pH _{ZPC} = 1.9 A _{SP} = 270 m ² g ⁻¹	Murray (1974), Catts and Langmuir (1986)	TLM ^d	6.40	-10.40	-7.95 ± 0.11	n.a.
			CCM (0.1 M)	(^f)	-2.14 ± 24.7	n.a.	n.a.
			DLM	(^f)	-3.27 ± 0.73	n.a.	n.a.
TiO ₂ (anatase)	pH _{ZPC} = 6.1 A _{SP} = (^g)	Berube and de Bruyn (1968), Sprycha (1984)	TLM ^d	-0.10	-3.9	-0.75 ± 0.84	n.a.
			CCM (0.1 M) ^e	6.64	-5.60	n.a.	n.a.
			DLM	5.37 ± 0.30	-5.92 ± 0.12	n.a.	n.a.
TiO ₂ (rutile)	pH _{ZPC} = 5.9 A _{SP} = 30 m ² g ⁻¹	Berube and de Bruyn (1968), Yates (1975)	TLM ^d	4.10	-8.10	7.13 ± 0.17	-4.59 ± 0.10
			CCM (0.1 M) ^e	3.91	-7.79	n.a.	n.a.
			DLM	4.23 ± 0.09	-7.49 ± 0.12	n.a.	n.a.
			TLM ^d	3.90	-7.90	5.24 ± 0.08	-6.42 ± 0.08

n.a. = parameters not applicable to CCM and DLM models.

^a N_S = 2.31 sites nm⁻² (from Dzombak and Morel, 1990) assumed for all minerals.

^b 95% confidence interval based on FITEQL standard deviation and defined using the methods of Dzombak and Morel (1990).

^c Mineral properties and DLM parameters for ferrihydrite are from Dzombak and Morel (1990).

^d For TLM, log K₊ and log K₋ fixed by convention. See text for discussion.

^e FITEQL did not converge at I = 0.1 M. Extrapolated from log₁₀(I) vs. log K₊ and log K₋.

^f Not considered for δ -MnO₂ and SiO_{2(amph)}.

^g The reported value of 16 m² g⁻¹ used with data of Sprycha (1984); 125 m² g⁻¹ used with data of Berube and de Bruyn (1968).

de Bruyn (1968) and Sprycha (1984) is so large (125 vs. $16 \text{ m}^2 \text{ g}^{-1}$) that the individual A_{SP} -values were maintained.

3.1. Site density (N_s)

Site densities reported for simple (hydr)oxides typically range between 1 and 20 sites nm^{-2} (Davis and Kent, 1990). Based on a literature survey, Dzombak and Morel (1990) recommended a total site density of 2.31 sites nm^{-2} for ferrihydrite. Since the goal of this study was a uniform application, the recommendation of Davis and Kent (1990) was followed and the site density of Dzombak and Morel (1990) was assumed for all minerals. Because there is no apparent physical reason for assuming different site densities for different models, the same site density has also been maintained for each SCM. Also implicit in the approach taken here is the equivalence of all sites. Since model simplification for PA is one desired goal of this study, and because of a lack of data on site heterogeneities for many of the minerals considered here, a single site type was assumed.

3.2. Capacitances

Capacitances for the CCM and TLM were selected based on the sensitivity analysis of Hayes et al. (1990). Capacitance for the CCM has been set at 1.0 F m^{-2} . For the TLM, the outer β -layer capacitance (C_2) has been set at 0.2 F m^{-2} and the inner α -layer capacitance (C_1) at 0.8 F m^{-2} . The DLM does not require capacitance values.

3.3. Chemical equilibrium model

The titration data selected for this study covered a range in ionic strength (I) from 0.0004 to 1 M . Using the approach outlined in Dzombak and Morel (1990), the mass action for the chemical equilibrium model at $I \leq 0.1 M$ was corrected for ionic strength effects using the Davies equation. At values greater than 0.1 M , activity coefficients were taken from Morel (1983). In this study, it was assumed that the solubility of the solids was negligible at the temperatures ($\sim 25^\circ\text{C}$) and times (minutes) being considered, and the chemical equilibrium model was not modified to consider dissolution of the solid.

For the DLM and CCM models, values for $\log K_+$ and $\log K_-$ were determined simultaneously using FITEQL. Because the TLM allows for sorption of the background electrolyte (e.g., Na^+ and NO_3^-), however, four equilibrium constants (K_+ , K_- , K_{cation} and K_{anion}) are necessary to describe the interface. In practice, FITEQL does not converge unless two of these can be specified. The relationship between K_+ , K_- , and zero point of charge (pH_{ZPC}) can be expressed:

$$(\log K_+ - \log K_-) / 2 = \text{pH}_{\text{ZPC}} \quad (6)$$

and the sensitivity analysis of Hayes et al. (1990) recommended a value for $\Delta \text{p}K$ such that:

$$\Delta \text{p}K = -[\log K_+ + \log K_-] = 4.0 \quad (7)$$

In this fashion, if pH_{ZPC} is known for a given mineral, values can be set for the TLM acidity constants and FITEQL can be used to solve for K_{cation} and K_{anion} . Values for mineral pH_{ZPC} were obtained from the open literature and are listed in Table 1.

Output from FITEQL includes a “goodness-of-fit” parameter (V_{γ}) and standard deviations for the estimated parameters (Westall, 1982). These values are determined based on the experimental error specified in the optimization run and the size of the data set. V_{γ} can be used as a measure of how well the data are described by the assumed chemical and adsorption models. Values between ~ 0.1 and ~ 20 are indicative of a good fit to the data, but in a strict sense V_{γ} cannot be compared directly unless the experimental error limits imposed on the problem are known. In most cases, however, error is not reported for potentiometric titration data, and the approach of Hayes et al. (1990) has been adopted. Relative error has been assumed to be $\pm 1\%$ (0.01), while absolute error has been assumed to be $1 \cdot 10^{-8} M$ instead of the $2 \cdot 10^{-8} M$ used by Hayes et al. (1990). Their sensitivity analyses indicated that the dissimilarities in acidity constants due to differences in experimental error are negligible, but the calculated uncertainty in the estimated values increases with increasing error.

Dzombak and Morel (1990) proposed a weighting scheme to combine results based on different data sets, relying on the standard deviation calculated by FITEQL. The weighted results are presented in Table 1. DLM and TLM values are based on combining values determined at different ionic strengths. Because it cannot account for changes in ionic strength, the values for the CCM are reported at $I = 0.1 M$ to establish a common reference point; the weighting scheme was applied if more than one analysis was available at this ionic strength. The 95% confidence limits (after Dzombak and Morel, 1990) are given in Table 1. Where it could be calculated, the uncertainty is much higher for the weighted CCM values than it is for the DLM and TLM. This is due to the smaller number of data sets available to be combined to yield the single ionic strength values ($I = 0.1 M$) reported for the CCM. Fig. 1 shows direct comparison of model results using weighted values from Table 1. All models proved capable of reproducing the observed data, with only slight differences. This is even true for goethite where data from five different studies were combined.

4. Radionuclide sorption on simple oxides: uranium sorption on goethite — an example

By establishing uniform values for N_{S} , K_{+} , K_{-} (and K_{cation} and K_{anion} for the TLM), only one adjustable parameter, the binding constant, remains for applying SCM's to radionuclide sorption. Uranium⁶⁺ [also UO_2^{2+} or U(VI)] sorption on goethite was used as a means of demonstrating procedures to determine radionuclide binding constants. With the input parameters developed above, FITEQL was used to model U(VI)–goethite sorption data reported by Tripathi (1984) and Hsi and Langmuir (1985).

In addition to data describing the mineral properties and the acid–base behavior of the surface (Table 1), FITEQL requires the input of a chemical equilibrium model for the system under investigation. For readily hydrolyzable elements such as UO_2^{2+} , the chemical system quickly becomes complicated with the inclusion of equilibrium con-

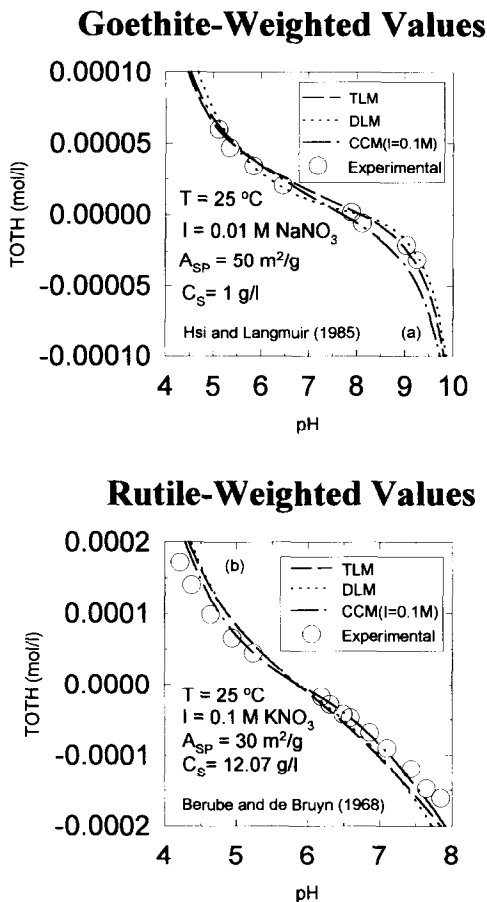


Fig. 1. Comparison of SCM modeling results for potentiometric titration data for: (a) goethite; and (b) rutile. Mineral properties and weighted values for K_+ and K_- (K_{cation} and K_{anion} for the TLM) from Table 1.

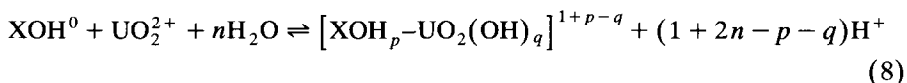
stants for the formation of aqueous species. For this reason, the resultant binding constants are dependent on the quality and extent of the thermodynamic data available for the system of interest. Implicit in this statement is that binding constants derived using FITEQL are only valid for the thermodynamic data used in constructing the chemical equilibrium model. For uranium, the equilibrium constants used in the chemical equilibrium models submitted to FITEQL were selected from the NEA Thermodynamic Database (Grenthe et al., 1992). All data were corrected for ionic strength effects ($I = 0.1 \text{ M}$ in these studies) using the Davies equation. If the same data sources are used, the binding constants can be applied in sorption/speciation codes such as MINTQA2 (Allison et al., 1991) to model uranium sorption once corrected to a reference state of $I = 0 \text{ M}$. Although analytical precision is sometimes given, total laboratory uncertainty is not generally reported. Where not reported, a data set was

assigned, perhaps optimistically, a relative error of $\sim \pm 1\%$ of the lowest measured amount. Relative error of ± 0.02 was assumed for pH. All standard deviations and uncertainties are reported relative to these values.

4.1. Controlled-atmosphere (no CO_2) experiments

The controlled-atmosphere data of Tripathi (1984) and Hsi and Langmuir (1985) demonstrate some of the challenges involved in interpreting radionuclide sorption data, particularly data from separate laboratories. The data of Hsi and Langmuir were measured with $[\text{U(VI)}]_{\text{T}} = 10^{-5} \text{ M}$, while the data of Tripathi consist of six sets of experiments, with $[\text{U(VI)}]_{\text{T}}$ ranging from $10^{-7.1}$ to $10^{-5.4} \text{ M}$. Both data sets were determined with 0.1 M NaNO_3 as a background electrolyte. The sorption edge of Hsi and Langmuir (1985) is ~ 1 pH unit lower than that of Tripathi (1984). This difference exceeds reported uncertainty in the analytical methods. Part of the discrepancy may be due to uranium loss to sinks other than goethite. Studies (Pabalan and Turner, 1993) report that potential uranium sinks in sorption experiments include the container walls, pipettes and filter assemblies. This loss is generally negligible at higher concentrations, but it can be significant for more dilute solutions in the range of 10^{-7} – 10^{-6} M . The data of Tripathi (1984) are corrected for losses to the container (polyethylene) walls, which shift the sorption edge down by as much as 20% for $[\text{U(VI)}]_{\text{T}} = 10^{-7.1} \text{ M}$ at $\text{pH} \approx 5.4$. The experiments of Hsi and Langmuir (1985) were also conducted in capped polyethylene bottles, but container loss cannot be accounted for in a quantitative way due to the lack of reported control data. In the absence of an objective way to select between the two available studies or a clear way to correct quantitatively for the different effects contributing to the discrepancies, it was decided to accept the experimental data as reported and compare modeling results.

Binding constants depend on the surface complex that is assumed to form. There are generally little independent data available on surface species and selecting an appropriate surface species is a subjective choice. In this system, uranium sorption was first modeled assuming monodentate complexation reactions involving only a single mononuclear uranyl-hydroxide species $[\text{UO}_2(\text{OH})_n^{2-n}]$:



Given the complex hydrolysis of U(VI), this is an oversimplification and the models could be further refined to better reproduce the data by invoking more than one surface complex, multidentate sorption, and/or consideration of polynuclear species such as was done by Kohler et al. (1992) and Payne et al. (1992). To satisfy the need to develop simple models for PA, the principle of parsimony has generally been adopted, and the simplest model capable of reproducing the observed data has been preferred.

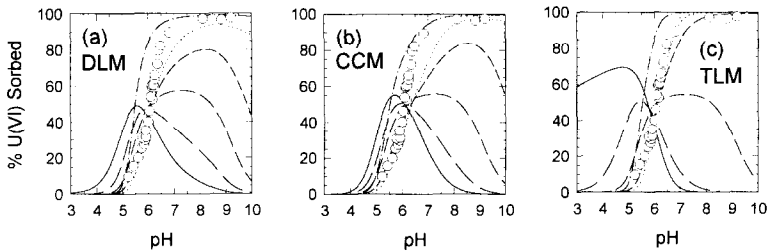
For the U(VI)– H_2O –goethite system (no CO_2), Table 2 lists binding constants determined for the sorption reactions using FITEQL. Results using weighted binding constants do not reproduce the observed sorption behavior nearly as well as the best-fit values, and illustrate one problem with combining data from different studies (Fig. 2). In

Table 2
Binding constants (log K) for forming the indicated surface complexes in the U(VI)–H₂O–goethite system (no CO₂)

Surfaces species	CCM			DLM			TLM		
	(TRI84) [±95%]	(H&L85) [±1σ]	(Wtd) [±95%]	(TRI84) [±95%]	(H&L85) [±1σ]	(Wtd) [±95%]	(TRI84) [±95%]	(H&L85) [±1σ]	(Wtd) [±95%]
XO–UO ₂ ⁺	1.29±0.15	2.69±0.04	1.65±0.25	1.82±0.15	3.13±0.04	2.15±0.24	-1.37±0.59	-2.51±0.04	-1.70±0.45
XOH–UO ₂ ²⁺	8.55±0.24	9.56±0.03	8.82±0.24	9.49±0.24	9.86±0.03	9.61±0.17	6.95±0.77	6.57±0.06	6.87±0.55
XO–UO ₂ OH ⁰	-5.94±0.09	-4.08±0.04	-5.50±0.31	-5.85±0.08	-3.76±0.04	-5.36±0.36	-7.61±0.27	-7.33±0.03	-7.53±0.19
XOH–UO ₂ OH ⁺	1.29±0.15	2.69±0.04	1.65±0.25	1.82±0.15	3.13±0.04	2.15±0.24	-0.04±0.81	0.97±0.04	0.23±0.59
XO–UO ₂ (OH) ₂ ⁻	-13.17±0.06	-10.77±0.04	-12.62±0.39	-13.54±0.05	-10.19±0.05	-12.89±0.50	-13.62±0.17	-11.38±0.05	-13.12±0.37
XOH–UO ₂ (OH) ₂ ⁰	-5.94±0.09	-4.08±0.04	-5.50±0.31	-5.85±0.08	-3.76±0.04	-5.36±0.36	-5.80±0.09	-3.99±0.04	-5.37±0.30
XOH ₂ –UO ₂ (OH) ₂ ⁺	1.29±0.15	2.69±0.04	1.65±0.25	1.82±0.15	3.13±0.04	2.15±0.24	2.32±0.19	4.29±0.05	2.76±0.34
XOH–UO ₂ (OH) ₃ ⁻	-13.17±0.06	-10.77±0.04	-12.62±0.39	-13.54±0.05	-10.19±0.05	-12.89±0.50	-11.87±0.06	-7.98±0.05	-11.03±0.61
XOH ₂ –UO ₂ (OH) ₃ ⁰	-5.94±0.09	-4.30±0.04	-5.50±0.31	-5.85±0.08	-3.76±0.04	-5.36±0.36	-4.07±0.04	-0.55±0.05	-3.30±0.55
XOH–UO ₂ (OH) ₄ ⁻	-20.35±0.06	-17.39±0.05	-19.68±0.47	-21.20±0.04	-16.80±0.06	-20.40±0.64	-17.70±0.16	-11.40±0.07	-16.39±1.97
XOH ₂ –UO ₂ (OH) ₄ ⁻	-13.17±0.06	-10.88±0.04	-12.62±0.39	-13.54±0.05	-10.19±0.05	-12.89±0.50	-10.15±0.05	-4.50±0.06	-8.97±0.87

Values calculated using FITEQL, Version 2.0 (Westall, 1982) with mineral properties and acidity constants listed in Table 1. Values corrected to $I = 0$ M using Davies equation. For data from TRI84 (Tripathi, 1984), $[U(VI)]_T = 10^{-5.4}$, $10^{-5.8}$, $10^{-6.0}$, $10^{-6.4}$, $10^{-6.7}$ and $10^{-7.1}$ M and uncertainties reflect 95% confidence limits determined using methods discussed in Dzombak and Morel (1990). For data from H&L85 (Hsi and Langmuir, 1985), $[U(VI)]_T = 10^{-5.0}$ M, and uncertainties are one standard deviation ($\pm 1\sigma$) as reported by FITEQL. Data are combined and 95% confidence limits determined using techniques from Dzombak and Morel (1990).

Tripathi (1984): $U(VI)_T = 10^{-6}$ M, 0.1 M $NaNO_3$, No CO_2 , $c_S = 0.41$ g/l



Hsi and Langmuir (1985): $U(VI)_T = 10^{-5}$ M, 0.1 M $NaNO_3$, No CO_2 , $c_S = 1$ g/l

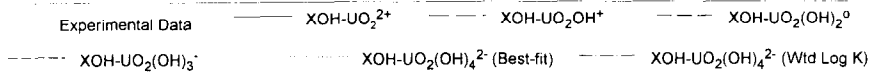
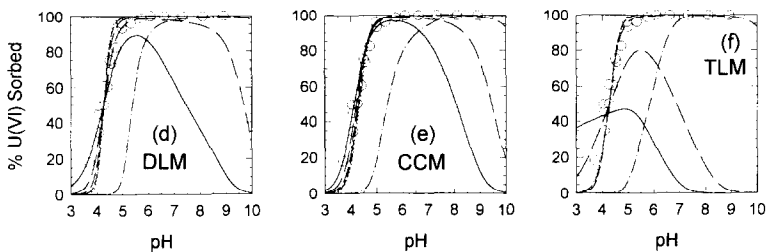


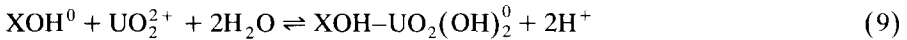
Fig. 2. SCM modeling results for $U(VI)-H_2O$ -goethite (no CO_2) system: (a) DLM; (b) CCM; and (c) TLM (data from Tripathi, 1984); and (d) DLM; (e) CCM; and (f) TLM (data from Hsi and Langmuir, 1985). Parameters from Tables 1 and 2.

this case, the binding constants based on the data of Tripathi (1984) for six uranium concentrations cluster at one set of lower values as compared to those derived from the single concentration reported by Hsi and Langmuir (1985). This is due to a need to push the modeled sorption edge to higher pH to match the data of Tripathi (1984) (Fig. 2); assuming formation of a single surface complex, smaller log K can accomplish this. All things being equal, the weighted constants exhibit a bias towards the values of Tripathi due to the relative sizes of the data sets, which is reflected in the model results (Fig. 2).

In addition to variations between data sets, it is apparent that resultant values are model-dependent. Because both protonation and deprotonation of surface sites and specific adsorption of uranyl (UO_2^{2+}) species are assumed to occur in the same plane for the DLM and CCM, the electrostatic correction is the same for like-charged surface complexes. As a result, if unit activity is assumed for H_2O , the estimated binding constants are the same (e.g., the log K is identical for $XOH-UO_2(OH)_2^0$ and $XO-UO_2OH^0$).

The modeling results (Fig. 2) for the data of Tripathi (1984) only reproduce observed sorption behavior assuming formation of $XOH-UO_2(OH)_4^{2-}$. This is surprising since $UO_2(OH)_4^{2-}$ is not predicted as an aqueous species below pH of ~ 12 . This suggests that hydrolysis may occur much more readily at the mineral-water interface, though independent data such as proton-release or extended X-ray absorption fine structure

spectroscopic (EXAFS) work are necessary to confirm these results. In contrast, the sorption behavior observed by Hsi and Langmuir (1985) is reproduced very well assuming a single surface complex of either $\text{XOH-}\text{UO}_2(\text{OH})_2^0$, $\text{XOH-}\text{UO}_2(\text{OH})_3^-$, or $\text{XOH-}\text{UO}_2(\text{OH})_4^{2-}$. There is a slight tailing of sorption at $\text{pH} > 9$ for $\text{XOH-}\text{UO}_2(\text{OH})_2^0$, consistent with experimental observations (Hsi and Langmuir, 1985). In addition, data from Hsi and Langmuir (1985) indicated that between 2 and 2.66 protons (H^+) were released for each uranyl ion adsorbed, suggesting that perhaps the neutral surface complex formed according to the reaction:



is most appropriate. It is important to remember, however, that in addition to reaction (9), the formation of $\text{XO-}\text{UO}_2\text{OH}^0$ and $\text{XOH}_2\text{-}\text{UO}_2(\text{OH})_3^0$ also releases two protons. As discussed above, the single-layer DLM and CCM cannot distinguish between reactions forming these three neutral surface species, and the fits will be identical to that shown in Fig. 2.

4.2. Modeling sorption in the U(VI)-H₂O-CO₂-goethite system

Similar to other actinide sorption experiments, the data of Tripathi (1984) and Hsi and Langmuir (1985) show that introduction of $\text{CO}_2/\text{CO}_3^{2-}$ leads to development of a desorption edge at higher pH (Fig. 3). This desorption has been attributed to both competition for sites by CO_3^{2-} and HCO_3^- (LaFlamme and Murray, 1987) and the competition for uranium by uranyl-(hydroxy)-carbonate complexes (Tripathi, 1984; Kohler et al., 1992). Recent work by Bruno et al. (1992) indicates that CO_2 and HCO_3^- interactions are strong at the hematite-water interface at CO_2 partial pressures (p_{CO_2}) of 0.97 and 0.30 atm. Zachara et al. (1987) also suggested that sorption of CO_3^{2-} , HCO_3^- and H_2CO_3^0 reduces chromate (CrO_4^{2-}) adsorption at $p_{\text{CO}_2} = 10^{-2.46}$ atm, indicating that competition for sorption sites by carbonate species may be significant where p_{CO_2} is elevated. Dzombak and Morel (1990) concluded that CO_3^{2-} and HCO_3^- sorb only weakly if at all, unless total carbonate concentrations are much greater than those occurring in systems open to atmospheric CO_2 ($p_{\text{CO}_2} = 10^{-3.48}$ atm). Payne et al. (1992) were able to provide an excellent fit to U(VI)- CO_2 sorption data for ferrihydrite using the two-site double-diffuse layer model of Dzombak and Morel (1990) without invoking site competition by CO_3^{2-} and HCO_3^- . Finally, control experiments in Hsi (1981) were unable to detect sorption of carbon species on goethite at $C_T = 10^{-4}$ M. Given the relative scarcity of quantitative data for many minerals at low p_{CO_2} on CO_3^{2-} and HCO_3^- surface reactions, sorption of uranyl-(hydroxy)-carbonate complexes was investigated here, but site competition between U(VI) and carbon-bearing species was not invoked. As more quantitative data for other minerals at lower p_{CO_2} become available for interpretation using the approach described here, sorption reactions involving CO_3^{2-} and HCO_3^- will be added to the chemical equilibrium model.

As with the controlled-atmosphere experiments, the formation of a single monodentate surface complex was initially assumed. Postulated surface complexes include: $\text{XOH-}\text{UO}_2\text{CO}_3$, $\text{XOH}_2\text{-}\text{UO}_2(\text{CO}_3)_2^-$, $\text{XOH}_2\text{-}\text{UO}_2(\text{CO}_3)_3^{3-}$, $\text{XOH}_2\text{-}(\text{UO}_2)_2\text{CO}_3(\text{OH})_3^0$ and $\text{XOH-}\text{UO}_2(\text{OH})_4^{2-}$. Estimated binding constants are listed in Table 3. For the data

Tripathi (1984): $U(VI)_T = 10^{-6}$ M, 0.1 M $NaNO_3$, $p(CO_2) = 10^{-3.48}$ atm, $c_S = 0.41$ g/l

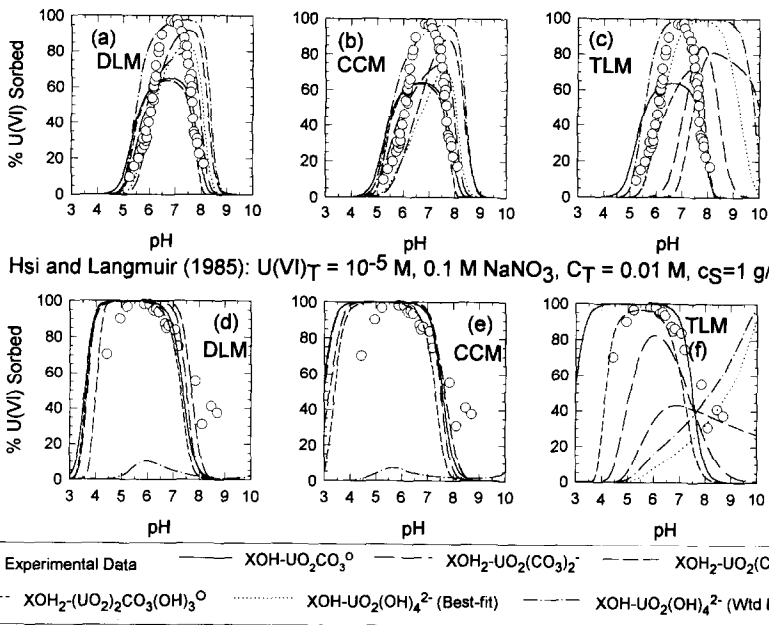


Fig. 3. SCM modeling results for U(VI)–H₂O–CO₂–goethite system: (a) DLM; (b) CCM; and (c) TLM (data from Tripathi, 1984); and (d) DLM; (e) CCM; and (f) TLM (data from Hsi and Langmuir, 1985). Parameters from Tables 1 and 3.

of Tripathi (1984), the assumption of a single surface complex was inadequate to model the observed behavior (Fig. 3). This is not surprising given the complexity of uranium speciation in the U(VI)–H₂O–CO₂ system and the added level of complexity in the observed sorption behavior. In general, the complexes that provide the best fit to the sorption/desorption edges fall short of the sorption maximum. If the sorption maximum is reached, the sorption envelope defined by the sorption and desorption edges tends to be too wide.

The sorption envelope defined by the data of Hsi and Langmuir (1985) is generally wider than that of Tripathi (1984) (Fig. 3). As a result, the calculated binding constants are typically larger (Table 3). As with the controlled-atmosphere experiments, the results of modeling the data of Hsi and Langmuir (1985) using the DLM and CCM are relatively insensitive to the postulated surface complex. All of the surface complexes match the sorption maximum (Fig. 3), but they tend to overpredict the sorption edge and underpredict the desorption edge. In addition, the models appear to impart too much pH dependence on the sorption behavior, leading to sorption/desorption edges that are steeper than observed.

Models can be improved for both data sets by postulating more than one surface species. For example, assuming a combination of the three surface species [XOH₂–

Table 3
Binding constants (log *K*) for forming the indicated surface complexes in the U(VI)–CO₂–H₂O–goethite system

Surface species	Binding constant (log <i>K</i>)			CCM			DLM			TLM		
	(TRI84) [± 95%]	(H&L85) [± 1σ]	(Wid) [± 95%]	(TRI84) [± 95%]	(H&L85) [± 1σ]	(Wid) [± 95%]	(TRI84) [± 95%]	(H&L85) [± 1σ]	(Wid) [± 95%]	(TRI84) [± 95%]	(H&L85) [± 1σ]	(Wid) [± 95%]
XOH–UO ₂ CO ₃ ⁰	15.88 ± 0.16	16.90 ± 0.03 (<i>C_T</i> = 10 ⁻³ M) 17.37 ± 0.06 (<i>C_T</i> = 10 ⁻² M)	16.22 ± 0.27	15.95 ± 0.15	17.50 ± 0.04 (<i>C_T</i> = 10 ⁻³ M) 17.03 ± 0.06 (<i>C_T</i> = 10 ⁻² M)	16.32 ± 0.30	16.03 ± 0.17	17.04 ± 0.03 (<i>C_T</i> = 10 ⁻³ M) 17.41 ± 0.05 (<i>C_T</i> = 10 ⁻² M)	16.38 ± 0.26			
XOH ₂ –UO ₂ (CO ₃) ₂ ⁻	30.16 ± 0.22	28.17 ± 0.02 (<i>C_T</i> = 10 ⁻³ M) 29.65 ± 0.05 (<i>C_T</i> = 10 ⁻² M)	29.51 ± 0.43	29.81 ± 0.21	27.71 ± 0.02 (<i>C_T</i> = 10 ⁻³ M) 29.26 ± 0.05 (<i>C_T</i> = 10 ⁻² M)	29.15 ± 0.45	31.97 ± 0.91	28.92 ± 0.03 (<i>C_T</i> = 10 ⁻³ M) 30.89 ± 0.04 (<i>C_T</i> = 10 ⁻² M)	30.94 ± 0.68			
XOH ₂ –UO ₂ (CO ₃) ₃ ³⁻	37.33 ± 0.25	39.32 ± 0.05 (<i>C_T</i> = 10 ⁻³ M) 35.30 ± 0.05 (<i>C_T</i> = 10 ⁻² M)	37.34 ± 0.58	36.08 ± 0.14	39.99 ± 0.07 (<i>C_T</i> = 10 ⁻³ M) 34.04 ± 0.06 (<i>C_T</i> = 10 ⁻² M)	36.28 ± 0.78	40.47 ± 2.90	52.30 ± 0.11 (<i>C_T</i> = 10 ⁻³ M) 38.41 ± 0.07 (<i>C_T</i> = 10 ⁻² M)	41.99 ± 2.52			
XOH ₂ –(UO ₂) ₂ ⁻ CO ₃ (OH) ⁰	11.72 ± 0.20	13.85 ± 0.06 (<i>C_T</i> = 10 ⁻³ M) 15.10 ± 0.09 (<i>C_T</i> = 10 ⁻² M)	12.50 ± 0.59	11.78 ± 0.21	14.45 ± 0.07 (<i>C_T</i> = 10 ⁻³ M) 15.13 ± 0.09 (<i>C_T</i> = 10 ⁻² M)	12.62 ± 0.64	13.22 ± 0.54	17.56 ± 0.07 (<i>C_T</i> = 10 ⁻³ M) 15.77 ± 0.07 (<i>C_T</i> = 10 ⁻² M)	14.60 ± 0.84			
XOH–UO ₃ (OH) ₂ ²⁻	-20.48 ± 0.20	-17.63 ± 0.06 (<i>C_T</i> = 10 ⁻³ M) -22.47 ± 0.05 (<i>C_T</i> = 10 ⁻² M)	-20.41 ± 0.71	-21.47 ± 0.17	-16.97 ± 0.08 (<i>C_T</i> = 10 ⁻³ M) -23.14 ± 0.05 (<i>C_T</i> = 10 ⁻² M)	-21.23 ± 0.83	-17.63 ± 0.37	-11.66 ± 0.10 (<i>C_T</i> = 10 ⁻³ M) -17.04 ± 0.06 (<i>C_T</i> = 10 ⁻² M)	-16.55 ± 1.01			

Values calculated using FITEQL, Version 2.0 (Westall, 1982) with mineral properties and acidity constants listed in Table 1. Values corrected to *I* = 0 M using Davies equation. For data from TRI84 (Tripathi, 1984), [U(VI)]_T = 10^{-5.4}, 10^{-5.8}, 10^{-6.0} and 10^{-6.7} M, and *p*CO₂ = 10^{-3.48} atm. Uncertainties reflect 95% confidence limits determined using methods discussed in Dzombak and Morel (1990). For data from H&L85 (Hsi and Langmuir, 1985), [U(VI)]_T = 10^{-5.0} M, and *C_T* = 10⁻³ and 10⁻² M. Uncertainties are one standard deviation (± 1σ) as reported by FITEQL. Data are combined and 95% confidence limits determined using techniques from Dzombak and Morel (1990).

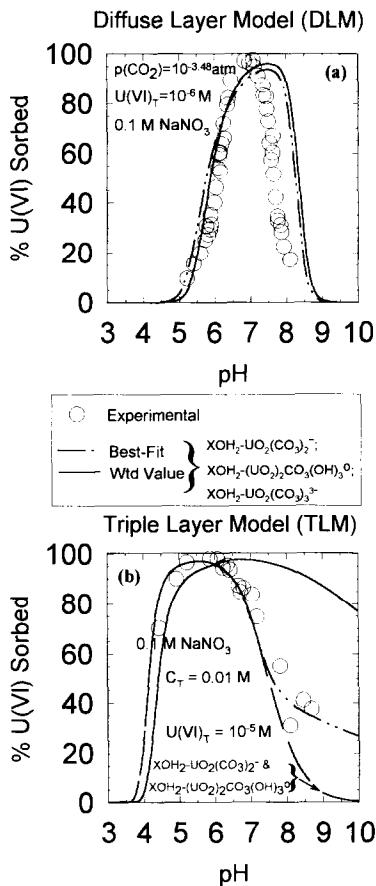


Fig. 4. SCM modeling results for the U(VI)–H₂O–CO₂–goethite system assuming three surface complexes: $\text{XOH}_2\text{-UO}_2(\text{CO}_3)_2^-$, $\text{XOH}_2\text{-UO}_2(\text{CO}_3)_3^{3-}$ and $\text{XOH}_2\text{-(UO}_2)_2\text{CO}_3(\text{OH})_3^0$: (a) DLM with data from Tripathi (1984), log *K* from Tables 1 and 3; and (b) TLM with data from Hsi and Langmuir (1985). The *short-dashed line* represents modeling assuming only $\text{XOH}_2\text{-UO}_2(\text{CO}_3)_2^-$ and $\text{XOH}_2\text{-(UO}_2)_2\text{CO}_3(\text{OH})_3^0$ as surface species; log *K* from Tables 1 and 3.

($\text{UO}_2)_2\text{CO}_3(\text{OH})_3^0$, $\text{XOH}_2\text{-UO}_2(\text{CO}_3)_2^-$ and $\text{XOH}_2\text{-UO}_2(\text{CO}_3)_3^{3-}$] results in a much closer fit (Fig. 4). Using the weighted values results in a slight improvement in the fit to the Tripathi (1984) data, but a significant deterioration in the fit to the data of Hsi and Langmuir (1985), which again shows the effects of the bias towards the larger data set of Tripathi (1984). Although such approaches have been demonstrated to provide an improved fit to the data set, it should be kept in mind that there is generally little information available on actual surface species. In addition, the added level of complexity introduced by multiple surface species may work against the practical application of SCM's in PA.

Table 4

Effect of data set size (number of measurements) on log K estimated using FITEQL

Surface Species	DLM: log K ($\pm 1\sigma$)			
	$m = 25$	$m = 13$	$m = 9$	$m = 5$
XO–UO ₂ ⁺	1.64 ± 0.04	1.62 ± 0.06	1.62 ± 0.07	1.58 ± 0.09
XOH–UO ₂ ²⁺	9.21 ± 0.04	9.16 ± 0.06	9.15 ± 0.08	9.10 ± 0.10
XO–UO ₂ OH ⁰	–5.97 ± 0.04	–5.96 ± 0.06	–5.94 ± 0.07	–6.01 ± 0.09
XOH–UO ₂ OH ⁺	1.64 ± 0.04	1.62 ± 0.06	1.62 ± 0.07	1.58 ± 0.09
XO–UO ₂ (OH) ₂ [–]	–13.65 ± 0.05	–13.64 ± 0.06	–13.62 ± 0.08	–13.66 ± 0.10
XOH–UO ₂ (OH) ₂ ⁰	–5.97 ± 0.04	–5.96 ± 0.06	–5.94 ± 0.07	–6.01 ± 0.09
XOH ₂ –UO ₂ (OH) ₂ ⁺	1.64 ± 0.04	1.62 ± 0.06	1.62 ± 0.07	1.58 ± 0.09
XOH–UO ₂ (OH) ₃ [–]	–13.65 ± 0.05	–13.64 ± 0.06	–13.62 ± 0.08	–13.66 ± 0.10
XOH ₂ –UO ₂ (OH) ₃ ⁰	–5.97 ± 0.04	–5.96 ± 0.06	–5.94 ± 0.07	–6.01 ± 0.09
XOH–UO ₂ (OH) ₄ ^{2–}	–21.32 ± 0.05	–21.31 ± 0.07	–21.30 ± 0.09	–21.32 ± 0.11
XOH ₂ –UO ₂ (OH) ₄ [–]	–13.65 ± 0.05	–13.64 ± 0.06	–13.62 ± 0.08	–13.66 ± 0.10

Data from Tripathi (1984). Mineral properties and acidity constants are listed in Table 1. Indicated uncertainties are one standard deviation ($\pm 1\sigma$) as reported by FITEQL. $[U(VI)]_T = 10^{-6} M$, no CO₂. Values corrected to $I = 0 M$ using Davies equation.

4.3. Effect of data set size

To evaluate the effect of the size of the data set, the controlled-atmosphere data of Tripathi (1984) for $[U(VI)]_T = 10^{-6} M$ was divided into progressively smaller subsets, and FITEQL was used to calculate DLM binding constants for the U(VI)–H₂O–goethite (no CO₂) system. The original 25 data points were arranged from lowest to highest pH; progressively smaller subsets were then extracted by selecting every other data point ($m = 13$ points), every third data point ($m = 9$) and every fifth data point ($m = 5$). All other parameters were held constant. Calculated log K -values for all surface complexes were similar for all subsets of the data (Table 4). However, as represented by the standard deviation calculated by FITEQL, the uncertainty in the value increased slightly with a decreasing number of data points. This is not surprising, as the geochemical system is less well constrained by a smaller data set. Although the uncertainty in the calculated binding constants is slightly greater for smaller data sets, it is not excessive and does offer some guidance in the ability to predict complex sorption behavior with a reasonable number of data points. However, it is critical that experiments be performed over a broad enough range in pH to adequately “sample” all aspects of the sorption behavior under consideration, especially in the presence of inorganic ligands such as carbonate.

4.4. Modeling of complex rock-forming minerals

Recent studies (e.g., Kohler et al., 1992) have proposed modeling radionuclide sorption on complex rock-forming minerals assuming a heterogeneous surface composed of stoichiometric proportions of sites such as silanol (SiOH⁰) and aluminol (AlOH⁰). U(VI)–kaolinite sorption (Payne et al., 1992) and Np(V)–biotite sorption (Nakayama

Table 5

log K -values the DLM for forming the indicated surface complexes in the U(VI)–kaolinite (Payne et al., 1992) and Np(V)–biotite (Nakayama and Sakamoto, 1991)

U(VI)–kaolinite (Payne et al., 1992)		Np(V)–biotite (Nakayama and Sakamoto, 1991)	
Surface complex	DLM: log $K^{(a)}$	Surface complex	DLM: log $K^{(a)}$
SiOH ₂ ⁺	n.a.	SiOH ₂ ⁺	n.a.
AlOH ₂ ⁺	8.33 ± 0.15	AlOH ₂ ⁺	8.33 ± 0.15
SiO ⁻	-7.20 ± 0.05	SiO ⁻	-7.20 ± 0.05
AlO ⁻	-9.73 ± 0.12	AlO ⁻	-9.73 ± 0.12
SiO–UO ₂ ⁺	0.96 ± 0.04	SiOH–NpO ₂ ⁺	2.86 ± 0.06
AlO–UO ₂ ⁺	2.18 ± 0.10	AlOH–NpO ₂ ⁺	4.15 ± 0.03
SiOH–UO ₂ ²⁺	5.73 ± 0.16	SiO–NpO ₂ OH ⁻	-11.58 ± 0.02
AlOH–UO ₂ ²⁺	9.20 ± 0.03	AlO–NpO ₂ OH ⁻	-12.39 ± 0.17
SiO–UO ₂ OH ⁰	-5.84 ± 0.44	-	-
AlO–UO ₂ OH ⁰	-4.74 ± 0.59	-	-

Acidity constants are from Table 1. $A_{sp} = 11 \text{ m}^2 \text{ g}^{-1}$ for kaolinite (Allard et al., 1983) and $8 \text{ m}^2 \text{ g}^{-1}$ for biotite. Except as noted, indicated uncertainties are one standard deviation ($\pm 1\sigma$) as reported by FITEQL. $[U(VI)]_T = 10^{-6} \text{ M}$; $[Np(V)]_T = 6 \cdot 10^{-6} \text{ M}$. Values corrected to $I = 0 \text{ M}$ using Davies equation. n.a. = $\text{pH}_{ZPC} \approx 2.8$ for SiO₂; SiOH₂⁺ not considered in this pH range.

^a Reported uncertainties represent 95% confidence limit for acidity constants. For surface complexes, listed uncertainty represents standard deviation ($\pm 1\sigma$) reported by FITEQL.

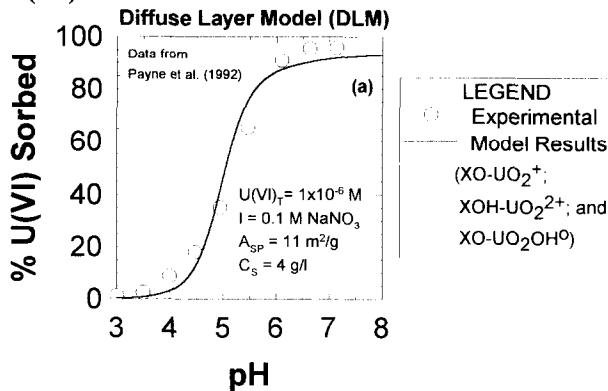
and Sakamoto, 1991) were investigated using this approach. Stoichiometries for kaolinite $[\text{Al}_2\text{Si}_2\text{O}_5(\text{OH})_4]$ and biotite $[\text{K}(\text{Mg},\text{Fe})_3\text{AlSi}_3\text{O}_{10}(\text{OH})_2]$ yield AlOH⁰/SiOH⁰ ratios of 1:1 and 1:3, respectively. Acidity constants from Table 1 for SiO₂ and $\alpha\text{-Al}_2\text{O}_3$ were used in these proportions. Binding constants were determined using FITEQL (Table 5).

Contaminant speciation (especially for actinides) varies rapidly as a function of pH; sorption edges that extend over wider pH ranges, such as those exhibited by the U(VI)–kaolinite and Np(V)–biotite data (Fig. 5), tend to require more than one surface complex (Dzombak and Morel, 1990). In all likelihood, the approach taken here is greatly simplified. For both sheet silicates, sorption behavior is probably due to a combination of ion exchange at intracrystalline sites and surface complexation along edge sites. In the U(VI)–kaolinite experiments, although there is no desorption edge over the pH range studied, the effects of carbonate may complicate interpretation of the results as discussed above. For Np(V)–biotite, the experiments are assumed to be CO₂ free, but other site types (e.g., Fe, Mg) probably also contribute to pH-dependent surface charge. Nevertheless, the relatively simple DLM is able to reproduce the observed behavior quite well (Fig. 5). However, as discussed earlier, the added complexity of multiple surface species tends to make the practical application of SCM's more difficult in PA.

5. Summary and conclusions

A first attempt has been made to develop and apply a consistent set of SCM parameters to radionuclide sorption. Using available potentiometric titration data,

U(VI) SORPTION ON KAOLINITE



Np(V) SORPTION ON BIOTITE

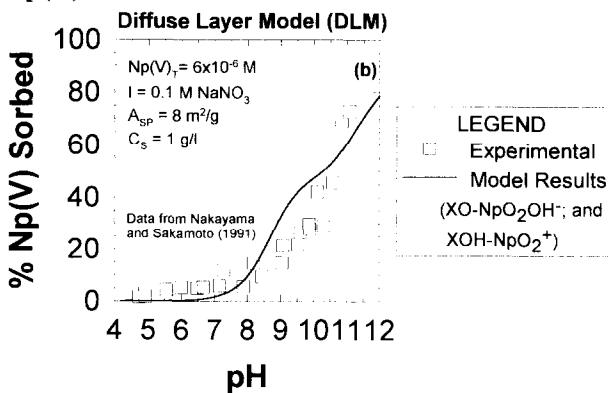


Fig. 5. DLM modeling results for: (a) U(VI)–kaolinite sorption (Payne et al., 1992); and (b) Np(V)–biotite sorption (Nakayama and Sakamoto, 1991). Postulated surface species are as indicated, binding constants are from Table 5.

model-specific values for K_+ , K_- , K_{cation} and K_{anion} have been developed for the CCM, DLM and TLM models using a uniform approach (Dzombak and Morel, 1990; Hayes et al., 1990). In general, all three models were able to simulate the observed acid–base behavior quite well. Only a single type of adjustable parameter, the binding constant, remains to model radionuclide sorption. It is important to remember, however, that in an effort to establish a baseline, the constants in Table 1 were determined using fixed site density, capacitances, and, in the case of the TLM, acidity constants. Although these parameters were selected based on surveys of mineral properties, they may not be the same as properties reported for a given set of experimental data. For this reason, results cannot be compared directly to constants determined using a different set of parameters. However, while there is some loss of conceptual (and numerical) accuracy in using a single set of parameters to model sorption data, this type of uniform approach

is to be favored in trying to strike a balance between model completeness and PA needs for efficient modeling.

The CCM is perhaps the most restrictive of the three models in that it requires knowledge of the dependence of capacitance on ionic strength. The TLM can model different ionic strengths, but it has a larger number of parameters and requires some means of fixing $\log K_+$ and $\log K_-$ to model titration data using FITEQL. This extra level of complexity tends to work against the ready incorporation of the TLM in PA calculations (Hayes et al., 1990). The simplest model, the DLM, is able to model ionic strength changes, and also has the fewest number of adjustable parameters and may be preferred.

U(VI) sorption on goethite (Tripathi, 1984; Hsi and Langmuir, 1985) was modeled to demonstrate the application of the approach to radionuclide sorption on simple hydr(oxides). Within the constraints of the conceptual model, the TLM was best able to model the CO₂-free data of Tripathi (1984) assuming a single XOH–UO₂(OH)₄²⁻ surface species. For the data of Hsi and Langmuir (1985), all three models proved capable of reproducing observed behavior; results were comparable for three different surface species. In the absence of independent data on actual surface species, proton release data suggest XOH–UO₂(OH)₂⁰ as a likely surface species.

Because of the twin constraints of sorption at low pH and desorption at higher pH, a single species is inadequate in most cases for U(VI)–goethite sorption in the presence of carbon-bearing species. Model results can be greatly improved by invoking additional species. This does not add significantly to the computational burden for geochemical modeling of static systems, but it may limit applications of SCM's to PA modeling of dynamic flow and transport.

As should be apparent from this study, development of a uniform set of radionuclide binding constants proceeds through a logical progression of steps from potentiometric titration data to radionuclide sorption data. Combining data from different laboratories may be problematic, and deciding between data sets is not always straightforward. This question is moot for many actinide–mineral systems, however, where only one set of experimental data is available. This effort has also pointed out inconsistencies in reporting data and experimental conditions in the literature. A number of data sets are not usable in this type of exercise merely because certain key pieces of information are missing. In addition, a more thorough reporting of experimental error would minimize the need to rely on assumed values; this would provide more accurate estimates for weighting factors.

The weighting scheme used allows for relatively easy updating of these data to incorporate new or revised data when they become available. Future efforts will concentrate on using these parameters in conjunction with the FITEQL code to model other available sorption data. In addition to simple (hydr)oxides, it should also be possible to apply these models to more complex rock-forming minerals as demonstrated for U(VI) sorption on kaolinite and Np(V) sorption on biotite. However, any radionuclide binding constants are dependent on the acidity constants used in the FITEQL optimization run; if these acidity constants are modified by the incorporation of new potentiometric titration data or changes in parameter values assumed while interpreting the present data, all radionuclide binding constants must be re-evaluated. In addition, the

tabulated binding constants are dependent on the thermodynamic data available. Any significant changes in the data likewise require a recalculation of the necessary parameters.

From the point of view of describing the mineral–water interface, it must be emphasized that the results given here are dependent on the assumptions used in constructing the conceptual model. Although some EXAFS data are available, due to analytical limitations they typically exist for fairly concentrated solutions (millimolar) at single pH-values. Additional EXAFS work will be required to ascertain the extent to which SCM's best represent the mineral–water interface. For the purposes of PA, a principle of parsimony was adopted in defining possible surface complexes in the U(VI)–H₂O–CO₂–goethite system. Within this framework, the DLM was able to reproduce the general aspects of uranyl sorption behavior while using a far simpler representation of the mineral–water interface than the TLM. This may be preferred where simpler models are desirable to strike a balance between accuracy of the conceptual model and the computational resources required by geochemistry in PA calculations.

Acknowledgements

This work was funded by the U.S. Nuclear Regulatory Commission (NRC), Office of Nuclear Regulatory Research, Division of Regulatory Applications (Dr. G. Birchard, project officer). This paper is an independent product of the Center for Nuclear Waste Regulatory Analyses (CNWRA) and does not necessarily reflect the views or regulatory position of the NRC. The calculational results presented were obtained using computer codes that are not currently in the CNWRA configuration management system. The authors would like to thank R. Pabalan and an anonymous reviewer for their thoughtful comments.

References

- Abendroth, R.P., 1970. Behavior of pyrogenic silica in aqueous electrolytes. *J. Colloid Interface Sci.*, 34: 591–596.
- Allard, B., Karlsson, M., Tullborg, E-L. and Larson, S.A., 1983. Ion exchange capacities and surface areas of some major components and common fracture filling materials of igneous rocks. Chalmers University of Technology, Göteborg, KBS 83-64, 61 pp.
- Allison, J.D., Brown, D.S. and Novo-Gradac, K.J., 1991. MINTEQA2/PRODEFA2 —A geochemical assessment model for environmental systems: Version 3.0 user's manual. U.S. Environ. Prot. Agency, Athens, GA, EPA/600/3-91/021, 106 pp.
- Balistrieri, L. and Murray, J.W., 1981. The surface chemistry of goethite (α -FeOOH) in major ion sea water. *Am. J. Sci.*, 281: 788–806.
- Berube, Y.G. and de Bruyn, P.L., 1968. Adsorption at the rutile–solution interface, 1. Thermodynamic and experimental study. *J. Colloid Interface Sci.*, 27: 305–318.
- Bolt, G.H., 1957. Determination of the charge density of silica soils. *J. Phys. Chem.*, 61: 1166–1169.
- Bruno, J., Stumm, W., Wersin, P. and Brandberg, F., 1992. On the influence of carbonate in mineral dissolution, I. The thermodynamics and kinetics of hematite dissolution in bicarbonate solutions at $T = 25^{\circ}\text{C}$. *Geochim. Cosmochim. Acta*, 56: 1139–1147.

- Catts, J.G. and Langmuir, D., 1986. Adsorption of Cu, Pb and Zn by δ -MnO₂: Applicability of the site binding surface complexation model. *Appl. Geochem.*, 1: 255–264.
- Davis, J.A., 1977. Adsorption of trace metals and complexing ligands at the oxide/water interface. Ph.D. Dissertation, Stanford University, Stanford, CA.
- Davis, J.A. and Kent, D.B., 1990. Surface complexation modeling in aqueous geochemistry. In: M.F. Hochella, Jr. and A.F. White (Editors), *Mineral–Water Interface Geochemistry*. Mineral. Soc. Am., *Rev. Mineral.*, 23: 177–260.
- Dzombak, D.A. and Morel, F.M.M., 1990. *Surface Complexation Modeling: Hydrous Ferric Oxide*. Wiley, New York, NY, 393 pp.
- Greenthe, I., Fuger, J., Lemire, R.J., Muller, A.B., Nguyen-Trung, C. and Wanner, H., 1992. *Chemical Thermodynamics Series, Volume 1: Chemical Thermodynamics of Uranium*. NEA (Nucl. Energy Agency), Elsevier, New York, NY.
- Hayes, K.F., Redden, G., Ela, W. and Leckie, J.O., 1990. Application of surface complexation models for radionuclide adsorption: Sensitivity analysis of model input parameters. USNRC (U.S. Nucl. Regulat. Comm.), Washington, DC, NUREG/CR-5547, 75 pp.
- Hsi, C-K.D., 1981. Sorption of uranium(VI) by iron oxides. Ph.D. Dissertation, Colorado School of Mines, Golden, CO.
- Hsi, C-K.D. and Langmuir, D., 1985. Adsorption of uranyl onto ferric oxyhydroxides: Application of the surface complexation site-binding model. *Geochim. Cosmochim. Acta*, 49: 1931–1941.
- Huang, C.P. and Stumm, W., 1972. The specific surface area of γ -Al₂O₃. *Surface Sci.*, 32: 287–296.
- Kohler, M., Wieland, E. and Leckie, J.O., 1992. Metal–ligand–surface interactions during sorption of uranyl and neptunyl on oxides and silicates. In: Y.K. Kharaka and A.S. Maest (Editors), *Proceedings of the 7th International Symposium on Water–Rock Interaction (WRI-7)*, Vol. 1: *Low Temperature Environments*. A.A. Balkema, Rotterdam, pp. 51–54.
- LaFlamme, B.D. and Murray, J.W., 1987. Solid/solution interaction: The effect of carbonate alkalinity on adsorbed thorium. *Geochim. Cosmochim. Acta*, 51: 243–250.
- Mesuere, K.L.G., 1992. Adsorption and dissolution reactions between oxalate, chromate, and an iron oxide surface: Assessment of current modeling concepts. Ph.D. Dissertation, Oregon Graduate Institute of Science and Technology, Beaverton, OR.
- Morel, F.M.M., 1983. *Principles of Aquatic Chemistry*. Wiley, New York, NY, pp. 446.
- Murray, J.W., 1974. The surface chemistry of hydrous manganese dioxide. *J. Colloid Interface Sci.*, 46: 357–371.
- Nakayama, S. and Sakamoto, Y., 1991. Sorption of neptunium on naturally-occurring iron-containing minerals. *Radiochim. Acta*, 52/53: 153–157.
- Pabalan, R.T. and Turner, D.R., 1993. Sorption modeling for HLW performance assessment. In: B. Sagar (Editor), *NRC High-Level Radioactive Waste Research at CNWRA January Through June 1993*. CNWRA (Cent. Nucl. Waste Regulat. Anal.), San Antonio, TX, CNWRA 92-02S: 8-1–8-18.
- Payne, T.E., Sekine, K., Davis, J.A. and Waite, T.D., 1992. Modeling of radionuclide sorption processes in the weathered zone of the Koongarra ore body. In: P. Duerden (Editor), *Alligator Rivers Analogue Project Annual Report, 1990–1991*. Aust. Nucl. Sci. Technol. Org., Canberra, A.C.T., pp. 57–85.
- Regazzoni, A.E., Blesa, M.A. and Maroto, A.J.G., 1983. Interfacial properties of zirconium dioxide and magnetite. *J. Colloid Interface Sci.*, 91: 560–570.
- Sprycha, R., 1984. Surface charge and adsorption of background electrolyte ions at anatase/electrolyte interface. *J. Colloid Interface Sci.*, 102: 173–185.
- Sprycha, R., 1989. Electrical double layer at alumina/electrolyte interface. *J. Colloid Interface Sci.*, 127: 1–11.
- Swallow, K.C., 1978. Adsorption of trace metals by hydrous ferric oxide. Ph.D. Dissertation, Massachusetts Institute of Technology, Cambridge, MA.
- Tripathi, V.S., 1984. Uranium(VI) transport modeling: Geochemical data and submodels. Ph.D. Dissertation, Stanford University, Stanford, CA.
- Westall, J.C., 1982. FITEQL: A computer program for determination of chemical equilibrium constants from experimental data, Version 2.0. Dep. Chem. Oregon State Univ., Corvallis, OR, Rep. 82-02, 61 pp.
- Westall, J.C. and Hohl, H., 1980. A comparison of electrostatic models for the oxide/solution interface. *Adv. Colloid Interface Sci.*, 12: 265–294.

- Yates, D.A., 1975. The structure of the oxide/aqueous electrolyte interface. Ph.D. Dissertation, University of Melbourne, Melbourne, Vic.
- Yates, D.A. and Healy, T.W., 1975. Mechanism of anion adsorption at the ferric and chromic oxide/water interfaces. *J. Colloid Interface Sci.*, 52: 222–228.
- Zachara, J.M., Girvin, D.C., Schmidt, R.L. and Resch, C.T., 1987. Chromate adsorption on amorphous iron oxyhydroxide in the presence of major groundwater ions. *Environ. Sci. Technol.*, 21: 589–594.